Alternative Models for Describing the Acid Unfolding of the Apomyoglobin Folding Intermediate[†]

Michael S. Kay and Robert L. Baldwin*

Department of Biochemistry, Stanford University Medical Center, Stanford, California 94305-5307

Received January 27, 1998; Revised Manuscript Received March 20, 1998

ABSTRACT: The acid-induced unfolding of the pH 4 intermediate of apomyoglobin (I) is described by either of two models: (1) a Monod−Wyman−Changeux-based model (MWC) where salt bridges perturb the pK_a values of specific ionizable side chains, causing unfolding of I as these salt bridges are broken at low pH, and (2) the Linderstrøm-Lang smeared charge model (L-L), which attributes acid unfolding of I to charge repulsion caused by the accumulation of positive charge on the surface of the protein. Both models fit earlier acid unfolding data well, but they make differing predictions about the effects of electrostatic mutants, which have been made and tested. Deletions of positive charge within I are found to stabilize I, but disruptions of potential salt bridges have little effect. These results show that the acid unfolding of I (I ⇌ U) is largely caused by generalized charge effects rather than by the loss of specific salt bridges. Acid unfolding of the native form, which is caused largely by a single histidine with a severely depressed pK_a, is a sensitive indicator of changes in stability produced by mutations. In contrast, the I ⇌ U transition is caused by a number of groups with smaller pK_a perturbations and both models predict that the pH midpoint of the I ⇌ U transition is an insensitive indicator of stability. This result reconciles previous conflicting results, in urea and acid unfolding studies of hydrophobic contact mutants, by showing that changes in the stability of I are poorly detected by acid unfolding.

The acid unfolding of apomyoglobin proceeds in two well-resolved steps from the native form (N) at pH 6 to the intermediate form (I) at pH 4 to the acid-unfolded form (U) at pH 2 (*1*). This three-state unfolding has been examined by numerous experimental and theoretical studies (*2−8*). These studies have suggested that the N to I transition is largely caused by the protonation of a buried, H-bonded pair of histidine residues (*5*), of which one histidine (H24) has a severely perturbed pK_a, with smaller contributions from other histidines as well as aspartates and glutamates with moderately perturbed pK_a values (*48*). Little experimental information is available, however, about the mechanism of the acid unfolding of I.

The apomyoglobin intermediate has been characterized in both equilibrium and kinetic studies. It is compact (*9,10*), formed rapidly from the acid-unfolded state (*8, 11*), and has three helices (A, G, and H) protected from hydrogen exchange (*6*) (see Figure 1). Recent NMR evidence from Wright and co-workers has shown that a portion of the B helix probably has loosely formed structure in I but minimal protection from hydrogen exchange (*12*). Previous studies have established that the B helix can be recruited to the intermediate by the addition of a stabilizing anion, TCA (*13*), and that mutagenesis of residues in the B helix affects the stability of I (*14*).

A previous study (*7*) examined the role of nativelike packing interactions in the stability of the acid intermediate
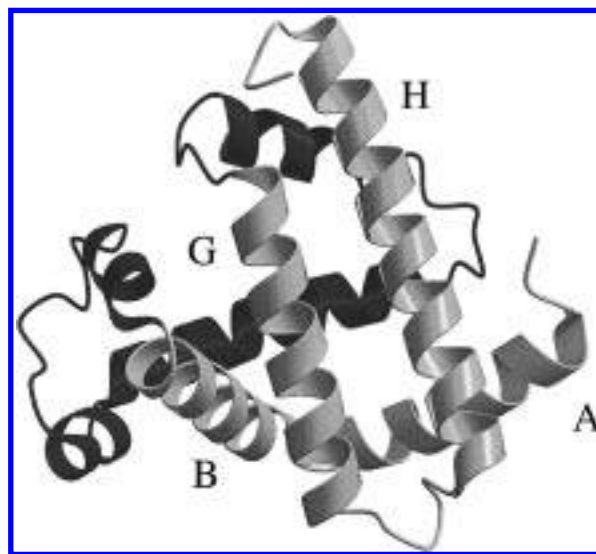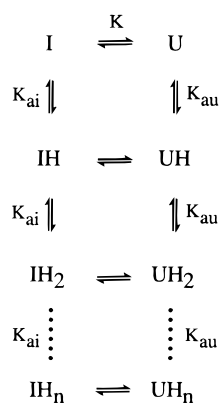

FIGURE 1: Ribbon diagram of myoglobin, with ABGH subdomain helices (gray) labeled. Created using Molscript (*45*) and Raster3D (*46, 47*).

by monitoring the pH midpoints of the N ⇌ I and I ⇌ U transitions in a series of nonpolar contact mutants. pH midpoint shifts were presumed to reflect changes in stability of the N and I forms. This study revealed large pH midpoint changes for the N ⇌ I transition but small changes for the I ⇌ U transition. The conclusion drawn from these results was that nativelike hydrophobic contacts, while very important for the stability of the native state, were relatively unimportant for the stability of the molten globule form (*4*). This conclusion left a conundrum about the nature of the acid intermediate's stabilization, because earlier studies (*4,*

* Corresponding author: Phone (650) 723-6169; FAX (650) 723-6768; E-mail kay@cmgm.stanford.edu.

Scheme 1: N Proton Binding Cycle Using MWC Model

$$
\begin{array}{ccc}
\text{I} & \overset{K}{\rightleftharpoons} & \text{U} \\
K_{ai} \updownarrow & & \updownarrow K_{au} \\
\text{IH} & \rightleftharpoons & \text{UH} \\
K_{ai} \updownarrow & & \updownarrow K_{au} \\
\text{IH}_2 & \rightleftharpoons & \text{UH}_2 \\
K_{ai} \vdots & & \vdots K_{au} \\
\text{IH}_n & \rightleftharpoons & \text{UH}_n
\end{array}
$$

7, 15) had shown that peptides with sequences corresponding to the A, G, and H helices do not form stable helices in isolation.

A more recent study (16) examined the role of nativelike buried hydrophobic interactions by urea-induced unfolding and found very significant destabilization caused by severe mutations. This study proposed a significant role for nativelike hydrophobic burial in the stabilization of I. We show here that the apparent discrepancy between these two studies on this important question stems from differences in the nature of the acid and urea unfolding.

In this work, we model the acid-induced I ⇌ U transition in either of two models: pK_a values of specific proton binding groups perturbed by salt bridges (Monod−Wyman−Changeux model) or generalized electrostatic repulsion (Linderstrøm-Lang model). Both these models fit the earlier data well. This modeling helps to explain the role of electrostatic interactions in causing unfolding of the molten globule as well as explaining the previous different conclusions drawn from urea and acid unfolding results. New electrostatic mutations are studied to test differing predictions of the two models; the results demonstrate that the acid unfolding of I can be largely attributed to a generalized charge effect rather than to the loss of specific salt bridges that stabilize I.

EXPERIMENTAL PROCEDURES

Models for Acid-Induced Unfolding. The Monod−Wyman−Changeux (MWC) model describes ligand-induced conformational transitions in terms of preferential binding of a ligand to specific groups (17). This model was originally applied to the cooperative binding of oxygen to hemoglobin but can be applied also to a folding transition caused by preferential binding of a ligand to the folded or unfolded state (e.g., refs 18 and 19). For acid-induced unfolding, the preferential binding of protons can be observed as lowered pK_a values of the contributing residues. A diagram of the MWC model applied to the binding of n protons is shown in Scheme 1.

The assumptions of the MWC model allow a simple description of a folding transition. All groups responsible for the transition are considered equivalent and independent. For the acid unfolding of the apomyoglobin intermediate, these assumptions correspond to equivalent pK_a values for all contributing groups and pK_a values that do not vary with titration of other ionizable groups. The transition is treated as two-state, with no populated intermediate states that are partly folded, partly unfolded. On the basis of these assumptions, the acid-induced unfolding curve depends solely on the number of ionizable groups involved (n), the pK_a values of these groups in I and U (pK_{aI} and pK_{aU}), and the stability of I when fully unprotonated (K). The final equation describing the acid-induced unfolding of I in terms of the fraction unfolded (F_u) is

$$
\frac{1}{F_u} = 1 + \frac{(1 + K_{aI}[H])^n}{K(1 + K_{aU}[H])^n} \tag{1}
$$

In contrast to the specific salt bridge interactions described by the MWC model, the Linderstrøm-Lang (L-L) smeared charge model attributes acid-induced unfolding to a bulk charge effect (20). As the pH is lowered, positive charge accumulates on the protein and destabilizes the compact structure by Coulombic repulsion. In this model, all charged groups contribute equally to the destabilization of the protein, and therefore, the stability of the protein is solely a function of its net charge. The L-L model also makes several simplifying assumptions. The charges are all treated equally and are considered to be distributed evenly over the surface of a sphere (the smeared charge approximation). This approximation has been shown to be inadequate for describing electrostatic interactions in native proteins (21). However, in a loosely structured "molten globule" folding intermediate, this description may be adequate, as supported by Goto and co-workers, who have shown that the stability of the partly reacted acid molten globule of cytochrome c depends solely on the its net charge (22, 23). These assumptions allow a simple description of the acid unfolding curve, using Debye−Hückel theory, solely as a function of N (the number of Asp and Glu groups whose pK_a is pK_{int} when the net charge, Z, is zero), Z_{max} (the net charge when all groups are protonated), the stability of I (ΔG), and w (which depends on the radius of the protein sphere and ionic strength).

The acid titration is described by (24)

$$
\log\left(\frac{\alpha}{1-\alpha}\right) = \text{pH} - pK_{int} + 0.868w(Z_{max} - \alpha N) \tag{2}
$$

where α is the fraction of the N groups not protonated at a given pH. Equation 2 describes the dependence of the net charge ($Z_{max} - \alpha N$) on pH. The dependence of ΔG on net charge is then given by

$$
\Delta G = \Delta G(0) - wRTZ^2 \tag{3}
$$

where $\Delta G(0)$ is the free energy of unfolding when the net charge (Z) is zero.

Analysis of Acid Unfolding Curves. To fit the acid unfolding titration curves of I with a minimum number of adjustable parameters, several constraints are required. First, as in previous work, the I ⇌ U transition is treated as two-state. There is considerable experimental evidence for this assumption, from both equilibrium and kinetic studies (11, 16). A recent study by Jamin and Baldwin (25) has shown that two forms of I (I_a and I_b) are present at low [urea], indicating that the I ⇌ U transition is not precisely two-state, but I_b is converted to I_a at low [urea] before the unfolding of I_a occurs. Related to the two-state assumption is the assignment of CD values for I and U. Analysis of the

I ⇌ U transition shows that I is fully populated at 0 M urea and the assignment for I is simply the CD measured at 0 M urea, averaging −14 000 deg cm^2 dmol^{-1} at 222 nm for the mutants studied here. The CD value of I at various urea concentrations is extrapolated using the baseline for fully folded I, as determined using the Santoro and Bolen procedure (*26*). The measured value for U is less straightforward. The measured CD value of U at 5 M urea (well after the end of the I ⇌ U transition) is near 0, reflecting a fully unfolded state devoid of helical structure. In contrast, for acid unfolding at pH 2, where the I ⇌ U transition is apparently complete, the CD value averages −4000 deg cm^2 dmol^{-1} (*3, 6*). The acid-unfolded and urea-unfolded forms of horse apomyoglobin also differ in their radius of gyration as measured by small-angle X-ray scattering (29.3 vs 34.2 Å) (*27*), indicating a more completely unfolded state in urea. Eliezer et al. (*12*) find significant residual helical structure in the pH 2 form. The CD value of U can be interpreted as (1) the CD value of the fully acid-unfolded state or (2) an equilibrium mixture of I and U (with zero CD), reflecting approximately 25% population of I at pH 2.

There are two lines of evidence that support the first interpretation. First, isolated peptides corresponding to the A, B, G, and H helices have small residual CD values, even at pH 2 (*4, 6, 14, 15*). The sum of their contributions at 222 nm at pH 2 is approximately −3250 deg cm^2 dmol^{-1}. The A helix, while not helical (as determined by its full far-UV spectrum), has a large aromatic far-UV signal that contributes significantly to the CD at 222 nm (*4*). Although other helices are not thought to be incorporated into I's compact structure, they are expected to have some residual helicity (*12, 28*) and contribute slightly to the overall CD content. It is reasonable to conclude that most, if not all, of the CD content of the acid-unfolded state comes from residual helicity and aromatic CD found in the isolated peptides rather than from a small population of I. Second, the CD value of the acid-unfolded state at pH 2 does not vary significantly with respect to changes in the stability of I (*16*). The CD value at pH 2 would be expected to drop significantly with destabilizing mutations if it is caused by the extent of populating I.

The acid-induced unfolding of I is also assumed to be solely caused by titration of Asp and Glu residues. This assumption is largely based on the pH midpoint of the transition (3.2). No other amino acids have intrinsic pK_as near this value. His (pK_a = 6.0) could contribute to the transition but would require a very large pK_a perturbation (>2 units) which, while possible for a native protein, is very unlikely in a marginally stable folding intermediate. A recent NMR study of the titration behavior of histidines in apoMb revealed that all histidines in I were fully protonated at pH 4, ruling out a large pK_a depression in I (*48*). Therefore, only Glu and Asp residues are expected to titrate and contribute to the acid-induced unfolding of I. For simplification of calculations, Glu and Asp residues are treated as a single type of amino acid.

Despite the simplicity of the two models, they contain many adjustable parameters, whose values are poorly determined by a single pH titration curve. These parameters can be constrained by known physical properties of I. The pK_a value of Asp/Glu in U (pK_{aU} or pK_{int}) should be near its value in unstructured peptide models (4.3 for Glu and 3.9

for Asp) (*29, 30*). In fitting the acid unfolding data, Glu and Asp are constrained to have a single pK_a value in U. The use of unstructured peptide models neglects small perturbations in pK_a caused by the significant amount of charge repulsion present in U at pH 2.0, or by traces of residual structure and compactness. Fersht and co-workers found that pK_a values in the acid-unfolded state of barnase are 0.4 unit lower than their reference values (*31*). For this work, we use a pK_{aU} value of 3.7 for Asp/Glu in U in the MWC model and a pK_{int} value of 4.0 (*24*) for the L-L model. The assigned values of pK_a and pK_{int} differ slightly because pK_{int} is defined as the pK_a in the absence of net charge.

Bipartite Nature of the Folding Intermediate. The pH 4 intermediate can be divided into two structural subdomains on the basis of hydrogen exchange protection data (*7, 13*). The A, G, and H helices are protected from exchange, while the remainder of the protein lacks significant protection. A recent report from Wright and co-workers suggests significantly populated helical structure in the B helix (*12*). Studies of helix propensity mutants in the B helix also show that it contributes to the stability of I (*14*). Initial studies of mutants outside this subdomain reveal little effect on the stability of I (*16*). On the basis of these data, the A, B, G, and H helices are treated here as the structured portion of the intermediate. The distribution of ionizable groups in I is shown in Table 1. Therefore, only ionizable groups within the A, B, G, and H helices are considered to contribute to the acid unfolding of I. In the Discussion, we consider the properties of the alternative model, which treats the electrostatic behavior of the entire molecule as being uniform.

Preparation of Proteins. Mutants were constructed starting from wt pMbT7 (*13*) using the MORPH site-directed mutagenesis kit from 5 Prime → 3 Prime, Inc. The synthetic myoglobin gene used here is from pMb413b, originally a gift from S. G. Sligar, University of Illinois (*32*). DNA sequences were confirmed by standard dideoxy methods at the Stanford Protein and Nucleic Acid Facility. Mutant and wt proteins were purified as described previously (*13*). Protein purity was >95% as judged by SDS−PAGE. Apomyoglobin stocks were prepared as previously described (*16*). Protein concentration was assayed by UV absorbance in 6 M guanidine hydrochloride [average of measurements at 280 nm (ϵ = 15 200 M^{-1} cm^{-1}) and 288 nm (ϵ = 10 800 M^{-1} cm^{-1}) (*33*)].

CD and Fluorescence Measurements. CD data were collected on an Aviv 62DS circular dichroism spectropolarimeter at 4 °C at 222 nm. All CD measurements were taken in a 1 cm × 1 cm quartz cuvette with approximately 2 μM apoMb. CD data was averaged over 300 s of acquisition time, after >10 min equilibration on ice. Fluorescence data was acquired on a SLM-Aminco Bowman Series 2 luminescence spectrometer in a 1 × 0.5 cm cell with 1 μM apoMb. All measurements were taken at 4 °C. All pH unfolding curves were measured in 2 mM citrate, while all urea unfolding curves were measured in 4 mM citrate, pH
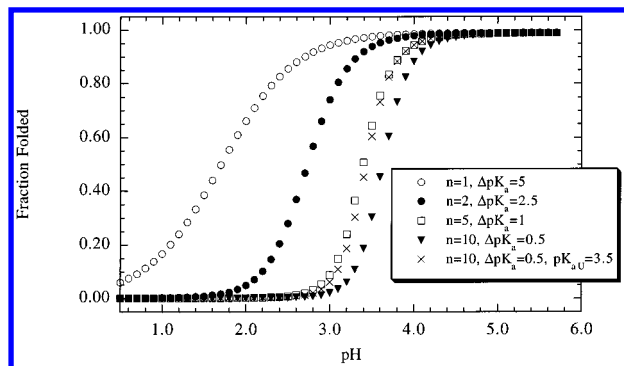
Table 1: Distribution of Charged Residues in Myoglobin

	Asp	Glu	Lys	His	Arg
Mb	7	14	19	12	4
ABGH	6	7	7	5	3
CDEF	1	7	12	7	1

FIGURE 2: Simulated pH titrations using MWC model for combinations of n and ΔpK_a ($n\Delta pK_a$ is fixed at 5), $pK_{aU} = 3.7$, $K = 0.01$.
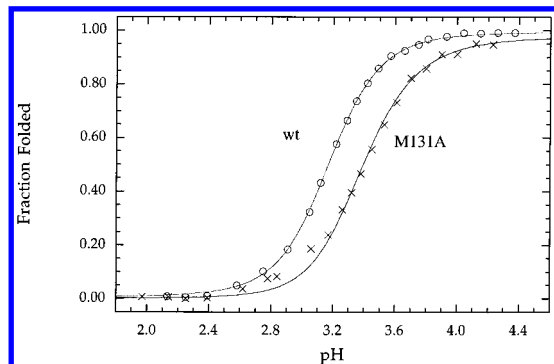

FIGURE 3: Best fits of MWC model for $n = 10$ to M131A and wt acid unfolding using floating pK_{aU} values (2 mM citrate, 4 °C) (see Results in text for parameters).

4.2 (additional citrate is needed to buffer concentrated urea solutions).

Analysis. All curve fitting was performed using Kaleida-Graph software for the Macintosh (Synergy Software). Correlation coefficients (R) are calculated in KaleidaGraph. Nonlinear fitting of pH titration data to the L-L model was performed using MATLAB for the Macintosh (The Math-Works). Urea unfolding data were fitted with linear baselines for I and U using the procedure of Santoro and Bolen (*26*). Acid unfolding data were fitted with a linear baseline for I but no baseline for U (because of insufficient data to determine a U baseline). Both pH and urea unfolding curves were normalized to remove baseline contributions and to fix the CD value of I to 1.0 and that of U to 0 (*16*).

Urea unfolding data for electrostatic mutants are reported as urea midpoint of unfolding (C_m). C_m is reported rather than ΔG to minimize the errors associated with long extrapolations back to 0 M urea and uncertainties in the poorly determined slope of the ΔG vs [urea] curve (*m* value) (*34, 35*). For illustrative purposes, these C_m values can be converted into ΔG values by using the average of all *m* values measured in this study (1500 cal/M).

RESULTS

MWC Modeling of the Acid Unfolding Data. The value of *n* is poorly determined by curve-fitting routines in the MWC equation, so it is assigned several discrete values, while the other parameters are permitted to float. The source of this uncertainty is the fact that *n* and ΔpK_a are tightly linked in the MWC model. For a given $n\Delta pK_a$, the shape of the titration curve will not vary significantly over a broad range of *n* (Figure 2), although the midpoint of the transition

will vary. Titration curves with constant $n\Delta pK_a$ can be superimposed by adjusting pK_{aU} (Figure 2) for $n \geq 4$.

The wt pH titration (Figure 3) can be fitted to the MWC model by fixing pK_{aU} (3.7) or allowing it to float. The best fit of the data from the MWC model with both methods gives the following parameters.

adjustable pK_{aU}

$n = 2$: no solution

$n = 4$: $pK_{aU} = 3.79$, $pK_{aI} = 2.52$, $K = 0.0030$; $\Delta pK_a = 1.27$

$n = 6$: $pK_{aU} = 3.56$, $pK_{aI} = 2.77$, $K = 0.0046$; $\Delta pK_a = 0.79$

$n = 8$: $pK_{aU} = 3.45$, $pK_{aI} = 2.88$, $K = 0.0052$; $\Delta pK_a = 0.57$

$n = 10$: $pK_{aU} = 3.39$, $pK_{aI} = 2.94$, $K = 0.0054$; $\Delta pK_a = 0.45$

fixed $pK_{aU} = 3.7$

$n = 2$: no solution

$n = 4$: $pK_{aI} = 2.40$, $K = 0.005$; $\Delta pK_a = 1.30$; $R = 0.99982$

$n = 6$: $pK_{aI} = 2.90$, $K = 0.002$; $\Delta pK_a = 0.80$; $R = 0.99971$

$n = 8$: $pK_{aI} = 3.09$, $K = 0.001$; $\Delta pK_a = 0.61$; $R = 0.99936$

$n = 10$: $pK_{aI} = 3.20$, $K = 0.0006$; $\Delta pK_a = 0.50$; $R = 0.99906$

With an adjustable pK_{aU}, all of the fits for values of *n* between 4 and 10 are of comparable quality ($R = 0.99983-0.99985$) and do not differentiate between the varying values of *n* (fit for $n = 10$ is shown in Figure 3). Some limits on *n* are evident, however, as the data are not compatible with a value of $n < 4$ (i.e., a small number of groups with large pK_a perturbations). The trend with increasing *n* is a decrease in pK_a value for U (ranging from 3.79 at $n = 4$ to 3.39 at $n = 10$) and an increase in the pK_a in I (2.52 at $n = 4$ to 2.94 at $n = 10$). The net result of these two trends is a nearly constant value for $n\Delta pK_a$ (5.1 at $n = 4$ to 4.5 at $n = 10$). The fitted values of *K* range between 0.0030 and 0.0054, near the urea measured value of 0.005 (*16*).

For a fixed value of pK_{aU}, there is a clear difference in the quality of the fits for varying *n*. The best fit is obtained for $n = 4$, with fits of decreasing quality for $n > 4$. In addition, the stability of I increases significantly with increasing *n*, such that for $n = 4$, the predicted *K* is similar to that observed in urea unfolding experiments (0.005) (*16*), while for $n = 10$ the predicted *K* is nearly 10-fold reduced. In these fits, the $n = 4$ fits are clearly superior to other values of *n*, in both quality of fit and the accurate prediction of stability of I. This set of fits shows that for a fixed value of pK_{aU}, a particular value of *n* can be obtained. In this set of fits, $n\Delta pK_a$ also remains nearly constant, ranging from 4.8 to 5.2.

The pH titration of a previously examined destabilizing hydrophobic contact mutant, M131A, is shown in Figure 3. According to the MWC model, in fitting the pH unfolding curve of nonelectrostatic mutants, only the stability of I

should vary, while the values of pK_{aI}, pK_{aU}, and n should remain constant. Retaining the values of the parameters obtained with the wt titration with the variable pK_{aU} fits, we can attempt to fit the mutant data (only allowing K to float). For $n = 4$ to $n = 10$, reasonable fits are obtained for M131A with the following parameters ($n = 10$ fit shown in Figure 3): for $n = 4$, $K = 0.011$; for $n = 6$, $K = 0.015$; for $n = 8$, $K = 0.018$; and for $n = 10$, $K = 0.019$. For pK_{aU} fixed to 3.7, a good fit is obtained for $n = 4$, $K = 0.018$.

The $\Delta\Delta G$ of the mutant in these fits is 0.7 kcal/mol, close to the value of 0.9 kcal/mol measured by urea unfolding. The quality of the fitting of the M131A data is not as good as for wt data because of the constraints of pK_{aU} and pK_{aI} to their wt values. At low pH, there is significant deviation from the fitted curve (Figure 3). If the pK_a values in I and U are permitted to float (data not shown), an excellent fit, comparable to the wt, is obtained with significantly higher pK_a values (for $n = 10$, $pK_{aI} = 3.32$ and $pK_{aU} = 3.76$). These fits of wt and M131A unfolding curves show that the MWC model can fit the I $\rightleftharpoons$ U transition reasonably well.

L-L Modeling of the Acid Unfolding Data. The L-L model also has several adjustable parameters that must be constrained to obtain meaningful fits of unfolding data. In contrast to the MWC model, three of these parameters have specific physical meanings (w, N, and Z_{max}). N corresponds to the number of titratable Asp and Glu groups in the ABGH subdomain (see Table 1). The ABGH subdomain has seven Glu and six Asp residues that titrate during the I $\rightleftharpoons$ U transition, giving a N of 13. The N- and C-termini are not included in the ABGH subdomain because they are unlikely to be structured in I (*12*). The total number of positive groups (Table 1) in the ABGH subdomain is 15 (seven Lys, five His, and three Arg). This distribution of charged residues means that the net charge in the ABGH subdomain will proceed from $+2$ ($Z_{max} - N$) to $+15$ (Z_{max}) during the pH titration. pK_{int} for Asp/Glu is set to 4.0 as discussed above.

The value of w is chosen on the basis of estimated physical properties of I. The radius of a slightly more structured intermediate, I_2 (formed in the presence of TCA), is 23 Å (*9*). The intermediate studied here is expected to be slightly less compact on the basis of its decreased hydrogen exchange protection, CD, and stability. For this study, we estimate a radius of 25 Å. The theoretical value of w can be calculated from

$$w = \frac{e^2}{2DkT}\left(\frac{1}{b} - \frac{\kappa}{1 + \kappa a}\right) \qquad (4)$$

where e = protonic charge, D = permittivity of water, k = Boltzmann's constant, T = temperature, b = radius of protein sphere, a = radius of salt exclusion ($b + 2.5$ Å), and $1/\kappa$ = Debye length (*21*). For $a = 25$ Å and $I = 0.002$, the calculated value of w is 0.12.

A minimum value of w for the I $\rightleftharpoons$ U transition may be calculated by using the simple observation that the apomyoglobin intermediate undergoes acid unfolding. For this unfolding to occur as a consequence of charge repulsion, the free energy of repulsion must significantly exceed the stability of the intermediate. For complete acid unfolding to be observed ($>95\%$), I must be at least 1.5 kcal/mol less stable than U ($\sim 3kT$) at the completion of the transition (pH
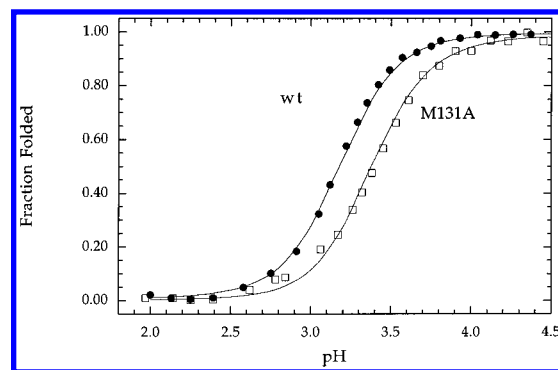

FIGURE 4: Best fits of L-L model to M131A and wt acid unfolding curves (2 mM citrate, 4 °C) for $w = 0.05$, $pK_{int} = 4.0$.
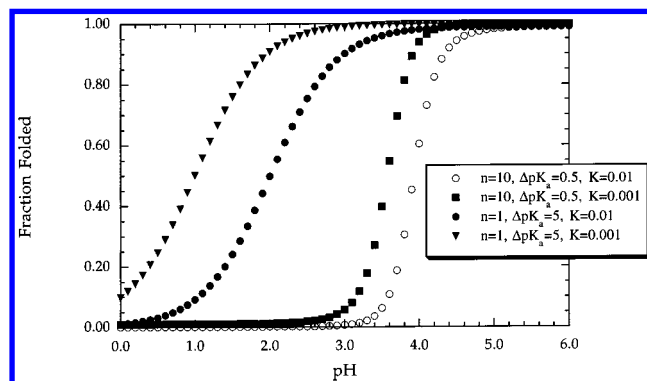

FIGURE 5: Simulated acid unfolding curves for two proteins differing in stability by 1.3 kcal/mol ($K = 0.01$ vs 0.001) using MWC model with $n = 1$, $\Delta pK_a = 5$ and $n = 10$, $\Delta pK_a = 0.5$ (constant $n\Delta pK_a$).

2). The electrostatic repulsion energy is given by $-wRTZ^2$, which corresponds to a minimum w-value of 0.04 at 4 °C. For simulations and fits of acid unfolding data, the w value will be allowed to vary between its minimum and maximum possible values (0.04 and 0.12).

The wt and M131A data are fitted well by $w = 0.05$ or 0.06. Fits with smaller w values are too broad, while fits with larger w values are too sharp (data not shown). The best fit of the L-L model with $w = 0.05$ and $pK_{int} = 4.0$ is shown in Figure 4. The fit parameters for $w = 0.05$ are $\Delta G(0) = 3.3$ kcal/mol for wt and 2.7 kcal/mol for M131A. Only $\Delta G(0)$ changes in fitting the mutant data. The ΔG values obtained from these fits should not be taken too seriously as the pH midpoint of the transition can be adjusted by changing either pK_{int} or $\Delta G(0)$ [e.g., a pK_{int} value of 3.7 results in a comparable fit with $\Delta G(0) = 2.5$ kcal/mol for wt and 1.9 kcal/mol for M131A]. A change of either of these parameters will move the titration curve to higher or lower pH without significantly altering the shape of the curve. However, the good fit of the shape of the curve with physically reasonable parameters supports the plausibility of the L-L model in this context.

Simulations. A major motivation of this study is to explain discrepancies between acid and urea unfolding data in previous mutant studies of the interactions stabilizing I. The fits of the MWC and L-L model to both wt and M131A data show that the small changes in pH midpoint observed in nonpolar contact mutants are compatible with significant changes in stability. To examine this effect clearly, Figure 5 shows MWC simulations of the acid unfolding of a 1.3 kcal/mol destabilizing mutant ($K = 0.01$ vs 0.001) with

Table 2: Acid and Urea Unfolding of Electrostatic Mutants

	ΔpH_{mid} I $\rightleftharpoons$ U[a]	$C_m{}^b$ (M urea)	$\Delta\Delta G$ (kcal/mol)
wt	0	1.56	0
R118A	−0.2	1.71	0.23
K133A	−0.1	1.89	0.49
R139A	−0.2	2.06	0.75
K140A	−0.1	1.76	0.30
K147A	−0.2	1.85	0.43
R31A	−0.2	1.82	0.39
H36Q	0[d]	1.49	−0.10
D20A	0	1.52 (1.42)[e]	0.06 (0.21)
D122A	0	1.56 (1.51)[e]	0 (0.07)

[a] Change in pH midpoint of I $\rightleftharpoons$ U transition from wild-type value of 3.2 (2 mM citrate, 4 °C) monitored by CD. [b] Stability of *I* measured by urea unfolding (4 mM citrate, pH 4.2, 4 °C) monitored by CD. [c] $\Delta\Delta G$ from wild-type value for average *m*-value of 1500. [d] Data from Barrick et al. (*5*). [e] Fluorescence-measured C_m values are shown in parentheses for D20A and D122A.

$n\Delta pK_a = 5$ ($n = 1$ and $\Delta pK_a = 5$ vs $n = 10$ and $\Delta pK_a = 0.5$). This simulation clearly shows that the pH midpoint is an insensitive indicator of stability changes when a large number of groups with small pK_a shifts are involved in the transition. In contrast, for transitions caused by a small number of groups with large pK_a changes, the pH midpoint faithfully reflects stability changes. In the example shown, the ΔpH_m is 0.35 for $n = 10$ and $\Delta pK_a = 0.5$ vs 1.0 for $n = 1$ and $\Delta pK_a = 5.0$. In the L-L model, the number of ionizable groups involved in the transition is not an adjustable parameter. The I $\rightleftharpoons$ U transition is always treated as being caused by a large number of groups with small pK_a perturbations. A simulated 1.3 kcal/mol mutant ($K = 0.01$ vs 0.001) results in a 0.4 unit pH_m shift (data not shown).

Electrostatic Mutants. To test the differing predictions of the two models (see Discussion), two classes of charge altering mutants were constructed. The first group targeted potential interhelical salt bridge interactions within I by alanine mutagenesis. A second group of mutants substituted alanine for positive residues not believed to be involved in interhelical salt bridges in order to change the net charge of the protein. Based on the crystal structure of myoglobin, there are four potential salt bridges between helices within the ABGH domain: Glu 6–Lys 133, Glu 105–Arg 139, Lys 16–Asp 122, and Asp 20–Arg 118. Previous theoretical studies have identified these salt bridges as contributing significantly to the stability of both N and I (*36–38*). Other charge-altering mutations were made at Lys 140 and 147 (surface of H helix) and Arg 31 (B helix). Lys 140 and Arg 31 have potential local electrostatic interactions with residues in their helices (i, $i + 4$), while Lys147 has no apparent electrostatic partner.

All mutants that delete a positive charge result in significant stabilization of I with ΔC_m of 0.15–0.50 M (0.2–0.75 kcal/mol) (Table 2 and Figure 6). The disruption of potential salt bridges (K133A, R139A, or R118A) did not result in destabilization. This result demonstrates that the removal of a single positive charge stabilizes I regardless of its location within the ABGH subdomain. For $w = 0.05$, the expected $\Delta\Delta G$ per charge at pH 4.2 is 0.3 kcal/mol. A previously studied charge mutant outside the ABGH subdomain, H36Q, has little effect on the stability of I (*5, 16*). The two mutants that remove a negative charge tested here, D20A and D122A, show little change in stability from wild
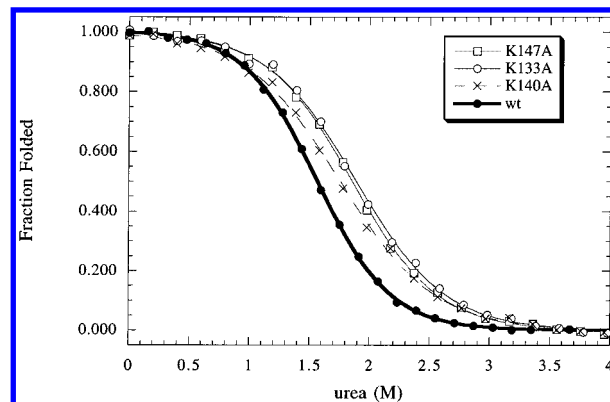

FIGURE 6: Representative normalized urea unfolding curves measured by CD of electrostatic mutants K133A, K140A, and K147A (pH 4.2, 4 mM citrate, 4 °C).
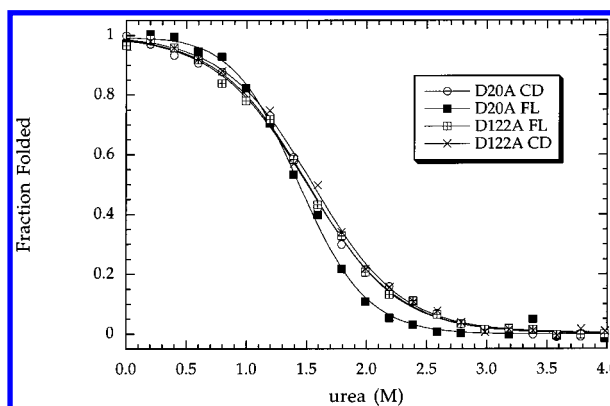

FIGURE 7: Normalized urea unfolding curves measured by CD and fluorescence of D20A and D122A (pH 4.2, 4 mM citrate, 4 °C).

type by CD-monitored urea unfolding (Table 2 and Figure 7). These two mutants have significantly broadened transitions, however, with elevated CD values at high [urea]. This pattern suggests a breakdown in the two-state unfolding of I, as has been observed previously for A130L (*16*). D20A and D122A were also studied by fluorescence to provide a second independent probe of unfolding. By fluorescence, D20A and D122A had decreased C_m values by 0.05 and 0.14 M (0.08 and 0.21 kcal/mol), respectively (Figure 7). The failure of the two-state assumption for these mutants is discussed below.

Stability of I at Higher pH. The MWC and L-L models also make predictions about the stability of I at higher pH (see Discussion). The L-L model predicts the presence of significant charge repulsion in I at pH 4.2. For the parameters giving the best fit of the wt data to the L-L model ($w = 0.05$ and $pK_{int} = 4.0$), a 0.8 kcal/mol electrostatic destabilization is predicted. This repulsion is predicted to be relieved by 0.6 kcal/mol by increasing the pH from 4.2 to 5.0. The MWC model predicts a similar increase in stability at pH 5 (magnitude increases with increasing n; at $n = 10$, $\Delta\Delta G = 0.8$ kcal/mol), because the salt bridges are not completely formed at pH 4.2. In wt apomyoglobin, I cannot be studied at a pH significantly higher than pH 4.2 because of the significant population of N. For H36Q, which destabilizes N but not I, the intermediate can be studied up to pH 5, however, without significant population of the native state. Urea denaturation of H36Q at pH 5 reveals a 0.78 M increase in C_m (1.2 kcal/mol) (Figure 8).
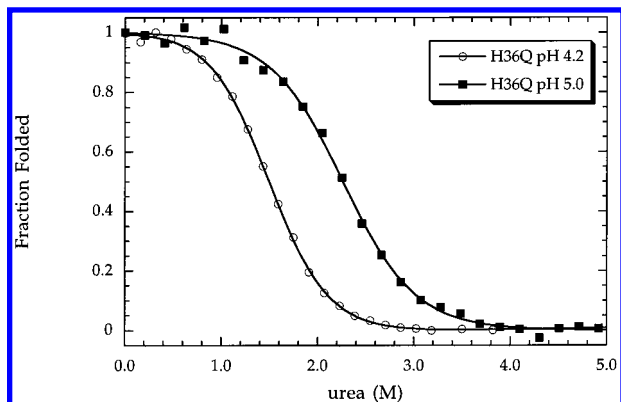
FIGURE 8: Normalized urea unfolding curves of H36Q at pH 4.2 and 5.0 (4 mM citrate, 4 °C).

DISCUSSION

In the present work, we have presented two models (MWC and L-L) to describe the acid-induced I $\rightleftharpoons$ U transition in apomyoglobin. Both models can be used to fit the pH unfolding curves of wt and a buried hydrophobic mutant, M131A, and predict that the I $\rightleftharpoons$ U transition is caused by numerous small pK_a perturbations. This property is the cause of insensitivity of the I $\rightleftharpoons$ U pH midpoint to changes in stability in I. The pH midpoint of the N $\rightleftharpoons$ I transition is more sensitive to destabilizing mutations because this transition has been shown to be largely caused by a single His residue with a >3 unit pK_a perturbation (*5, 39, 48*). This conclusion resolves the apparent contradiction between two previous studies (*7, 16*) by showing that acid-induced unfolding is an insensitive technique for studying stability changes in a weakly stable folding intermediate, as it depends on the magnitude of the pK_a perturbation as well as changes in stability.

Comparing the Two Models. Although both the MWC and L-L models fit the pH titrations of wt and M131A well, they make several differing predictions. The MWC model predicts that the I $\rightleftharpoons$ U transition is caused by the loss of stabilizing interactions between several distinct ionizable groups. These stabilizing interactions (salt bridges) lower the pK_a values of participating Asp and Glu residues. Loss of these salt bridges should decrease the stability of the intermediate (as tested by both urea- and acid-induced unfolding). In contrast, the L-L model states that the stability of the intermediate will depend solely on net charge, predicting that loss of positively charged residues will increase the stability of the intermediate by reducing charge repulsion, while loss of negatively charged residues will decrease stability.

Mutations of positive residues to alanine within the ABGH subdomain all stabilize I significantly (0.4−0.8 kcal/mol), regardless of whether they are involved in putative salt bridges. There is no mechanism within the MWC model to account for these results. This result also strongly suggests that salt bridges are energetically unimportant in stabilizing I. In contrast, these results are predicted qualitatively by the L-L model, since loss of a positive charge reduces the net charge in I and, therefore, is stabilizing. The magnitude of the stabilization induced by loss of a positive charge is significantly greater than predicted by our L-L simulation (0.3 kcal/mol). Part of this increase may be caused by the

high helix propensity of alanine. Lys and Arg both have strong helix propensities, however, and the expected size of this effect is not known.

There are several possible sources of uncertainty in fitting the acid unfolding data to the L-L model. Removal of a single positive charge at various sites in the ABGH subdomain causes variable increases in stability (0.23−0.75 kcal/mol), indicating that the assumption of identical and equivalent charged groups in I is not completely correct. Other sources of error involve the uncertainty of the *w* value and possible variability in the compactness of structure in various regions of I. Recent NMR studies (*12*) of I show significant fraying of all helices in I, such that all charged groups in these helices may not fully participate in the bulk electrostatic repulsion of the compact subdomain.

According to both models, loss of negatively charged groups in I should destabilize I, by loss of salt bridges (MWC) or increase in net positive charge (L-L). The experiments on Asp20 and Asp118 are, however, somewhat difficult to interpret because of the broadness of the urea-induced unfolding curve monitored by CD and the elevated residual helicity at high urea concentrations. Fluorescence-monitored unfolding of these mutants differs slightly from the CD-monitored unfolding. This pattern of disagreement suggests non-two-state behavior in these mutants. By CD, there is little change in the stability of I compared to wt, while fluorescence reports 0.1 (D122A) and 0.3 kcal/mol (D20A) destabilization. The deletion of a negative charge in I is also more difficult to interpret because Asp or Glu residues are expected to carry only partial charge at pH 4.2, whereas the loss of an Arg or Lys residue should result in the loss of a full charge.

Another prediction of the two models is the change in stability of I with increasing pH. H36Q, unlike wt, can be studied at pH 5, and I is essentially completely populated at both pH 4.2 and 5.0. The large increase in stability of H36Q measured at pH 5 supports the L-L model with its prediction of significant electrostatic repulsion in I at pH 4.2, which is relieved as Asp and Glu residues become fully charged. The MWC model predicts a similar stabilizing effect, as the Asp and Glu residues are only partially deprotonated at pH 4.2 and become fully charged with increasing pH. The magnitude of the stabilization observed is significantly larger than predicted by the L-L model, again showing that the quantitative details of the L-L model are not accurate. This result supports previous modeling (*3*) and kinetic hydrogen exchange data (*8*), which predict that I is more stable at higher pH.

The MWC model predicts that the addition of salt will destabilize I by screening favorable salt bridge interactions if they are surface-exposed. In contrast, the L-L model predicts that high ionic strength will stabilize I as a result of screening of charge repulsion of the charged residues. The effect of increasing ionic strength on I is difficult to study because of strong anion binding, which stabilizes I. Goto et al. (*40*) have shown that the addition of a variety of anions (e.g., chloride, sulfate, perchlorate, and TCA) induces the formation of I at pH 2. These anions also stabilize I to urea unfolding at pH 4.2 (*13, 34*). At pH 4.2, the addition of 0.5 M NaCl significantly stabilizes I (4.5 kcal/mol) (Kay and Baldwin, unpublished data). This stabilization may be

caused by either anion binding or screening of charge repulsion.

Detailed Evaluation of the L-L Model. From the discussion above, it is clear that the L-L model describes the acid-induced I $\rightleftharpoons$ U transition of apoMb much better than the MWC model. Although not quantitatively accurate in its predictions, the L-L model predicts the effects of all electrostatic mutants studied. Previous studies have established that the L-L model is an inadequate description of the pH-induced unfolding reactions of native proteins (*21*). A more precise electrostatic model based on the exact locations of charged groups and their solvent accessibility allows both stabilizing and destabilizing electrostatic interactions without invoking salt bridge formation (*41*) and more accurately models the pH-dependent stability of native proteins. Goto (*22, 23*) demonstrated, however, that the stability of the cytochrome *c* molten globule depends solely on the net charge and that the L-L model may adequately describe such species. In this work, Goto generated species with differing net charge by partially acetylating Lys groups and separating them by electrophoresis. Mixtures of proteins with a specific net charge were then studied by urea-induced unfolding. From his data, a *w* value of 0.02 can be calculated for the cytochrome *c* molten globule, based on the slope of the plot of free energy vs square of net charge. The estimated radius of the cytochrome *c* molten globule is 17 Å (from small-angle X-ray scattering). At $I = 0.018$, where Goto's studies are conducted, the calculated value of *w* (eq 3) is 0.12, well above the measured value. The calculated *w* value for apoMb I is 0.12, significantly higher than the best-fit value from pH titrations (0.05). The source of the difference between these calculated and measured *w* values may be related to the flexible nature of the molten globule intermediate, which is probably not completely impenetrable to solvent, unlike native proteins. The flexible nature of the molten globule may also dampen repulsion between positively charged groups, allowing small adjustments in tertiary structure. Another possible source of error is anion binding under the conditions of this study. The citrate buffer used here is known to bind to I and stabilize it. This binding should reduce the net charge in I, but the extent of this effect is unknown. The use of other noninteracting buffers gives poor resolution of the N $\rightleftharpoons$ I and I $\rightleftharpoons$ U transitions.

The assumption of bipartite structure in I is well supported by previous NMR (*12*), hydrogen exchange (*6, 13*), and mutagenesis studies (*16*). The precise borders of the structured areas in I are, however, unknown. The electrostatic mutations studied here show that all positive residues mutated within the ABGH subdomain decrease the stability of I. Although the evidence for inclusion of the A, G, and H helices in the intermediate is well-established (*4*), the inclusion of the B helix as part of I is a relatively recent concept, largely coming from recent NMR studies (*12, 13*) and a mutagenesis study of the B helix (*14*). R31A, in the B helix, significantly stabilizes I, supporting the inclusion of the B helix in the compact structure of I. A charge mutant previously studied (*5, 16*), H36Q, lies just outside the B helix and does not significantly affect the stability of I. This result argues against applying the L-L model to all charged residues in apomyoglobin. A corresponding study of mutated positive residues outside the ABGH subdomain is underway in this laboratory (Ramos, Kay, and Baldwin, unpublished results).

Comparisons with Previous Modeling. This work allows an initial experimental evaluation of the numerous previous theoretical studies on myoglobin. Many of these studies concern the native state of holomyoglobin, applying an electrostatic potential function to the molecular coordinates of holomyoglobin obtained from its crystal structure. Only recently has detailed structural information on N and I become available from NMR studies by Wright and co-workers (*12, 42*). A theoretical study of the acid unfolding of I (*38*) treated I as a fully structured subdomain of holomyoglobin and found that the transition was largely driven by a small number of carboxylate groups with unusually low pK_a values. The actual intermediate form is, however, significantly less structured than holoMb and it is expected to exhibit increased flexibility and solvent penetration compared to the native form, thus weakening specific salt bridge interactions. Because the tertiary structure of I is not as well-defined as in native proteins, fixing charged groups for a salt bridge interaction is also likely to result in a greater entropic penalty.

Hollecker and Creighton (*43*) performed charge altering studies on several native proteins to assess the role of net charge in the stability of native proteins. Their results showed that changing net charge (by random chemical modification of freely reacting amino groups) contributed little to the stabilities of the proteins, as measured by urea gradient electrophoresis. In several cases, sudden changes in stability were observed with one additional modification, implying the occasional importance of specific groups involved in strong electrostatic interactions. Their results contrast with Goto's data (*22, 23*) on the molten globule of cytochrome *c* and, together with the current work, show a clear difference in the mechanism of acid unfolding of native vs "molten globule" forms.

Recent studies from Brunori and co-workers (*44*) have shown that the distantly related *Aplysia* apomyoglobin undergoes a single unfolding transition (N $\rightleftharpoons$ I), in contrast to the three-state unfolding in sperm whale apomyoglobin. This difference in acid-unfolding behavior is attributed to the large difference in p*I* between sperm whale apoMb (8.9) and *Aplysia* apoMb (4.5). At pH 2, there is only a slight accumulation of positive charge in *Aplysia* apoMb, permitting population of its intermediate. These results support the smeared-charge model, implying that net charge, rather than specific electrostatic interactions, is the dominant source of changes in stability of I with pH.

The three-state model of Barrick and Baldwin (*3*) attributes the acid unfolding of apoMb to a small number of ionizable groups in both the N $\rightleftharpoons$ I and I $\rightleftharpoons$ U transitions. This model was designed to interpret the N $\rightleftharpoons$ I transition for histidine mutants and was used to identify the key His24–His119 interaction that is largely responsible for the N $\rightleftharpoons$ I transition. This model is very similar to the MWC model described here, except that the pK_a values of ionizable groups participating in either transition were treated as infinitely perturbed (i.e., titration of the group is incompatible with the structure of N or I) in order to minimize the number of adjustable parameters. This model describes the N $\rightleftharpoons$ I transition well because of the large pK_a shift of the His24. However, I is not capable of harboring such large pK_a perturbations, and the model is not applicable to the I $\rightleftharpoons$ U transition.

REFERENCES

1. Griko, Y. V., Privalov, P. L., Venyaminov, S. Y., and Kutyshenko, V. P. (1988) Thermodynamic study of the apomyoglobin structure, *J. Mol. Biol. 202*, 127−38.
2. Alonso, D. O., Dill, K. A., and Stigter, D. (1991) The three states of globular proteins: acid denaturation, *Biopolymers 31*, 1631−49.
3. Barrick, D., and Baldwin, R. L. (1993) Three-state analysis of sperm whale apomyoglobin folding, *Biochemistry 32*, 3790−6.
4. Barrick, D., and Baldwin, R. L. (1993) The molten globule intermediate of apomyoglobin and the process of protein folding, *Protein Sci. 2*, 869−76.
5. Barrick, D., Hughson, F. M., and Baldwin, R. L. (1994) Molecular mechanisms of acid denaturation. The role of histidine residues in the partial unfolding of apomyoglobin, *J. Mol. Biol. 237*, 588−601.
6. Hughson, F. M., Wright, P. E., and Baldwin, R. L. (1990) Structural characterization of a partly folded apomyoglobin intermediate, *Science 249*, 1544−8.
7. Hughson, F. M., Barrick, D., and Baldwin, R. L. (1991) Probing the stability of a partly folded apomyoglobin intermediate by site-directed mutagenesis, *Biochemistry 30*, 4113−8.
8. Jennings, P. A., and Wright, P. E. (1993) Formation of a molten globule intermediate early in the kinetic folding pathway of apomyoglobin, *Science 262*, 892−6.
9. Kataoka, M., *et al.* (1995) Structural characterization of the molten globule and native states of apomyoglobin by solution X-ray scattering, *J. Mol. Biol. 249*, 215−28.
10. Eliezer, D., *et al.* (1995) The radius of gyration of an apomyoglobin folding intermediate, *Science 270*, 487−8.
11. Jamin, M., and Baldwin, R. L. (1996) Refolding and unfolding kinetics of the equilibrium folding intermediate of apomyoglobin, *Nat. Struct. Biol. 3*, 613−8.
12. Eliezer, D., Yao, J., Dyson, H. J., and Wright, P. E. (1998) Structural and dynamic characterization of partially folded states of apomyoglobin and implications for protein folding, *Nat. Struct. Biol. 5*, 148−55.
13. Loh, S. N., Kay, M. S., and Baldwin, R. L. (1995) Structure and stability of a second molten globule intermediate in the apomyoglobin folding pathway, *Proc. Natl. Acad. Sci. U.S.A. 92*, 5446−50.
14. Kiefhaber, T., and Baldwin, R. L. (1995) Intrinsic stability of individual alpha helices modulates structure and stability of the apomyoglobin molten globule form, *J. Mol. Biol. 252*, 122−32.
15. Waltho, J. P., Feher, V. A., Merutka, G., Dyson, H. J., and Wright, P. E. (1993) Peptide models of protein folding initiation sites. 1. Secondary structure formation by peptides corresponding to the G- and H-helices of myoglobin, *Biochemistry 32*, 6337−47.
16. Kay, M. S., and Baldwin, R. L. (1996) Packing interactions in the apomyglobin folding intermediate, *Nat. Struct. Biol. 3*, 439−45.
17. Monod, J., Wyman, J., and Changeux, J. P. (1965) On the Nature of Allosteric Transitions: A Plausible Model, *J. Mol. Biol. 12*, 88−118.
18. Sage, J. T., Morikis, D., and Champion, P. M. (1991) Spectroscopic studies of myoglobin at low pH: heme structure and ligation, *Biochemistry 30*, 1227−37.
19. Morikis, D., Champion, P. M., Springer, B. A., and Sligar, S. G. (1989) Resonance Raman investigations of site-directed mutants of myoglobin: effects of distal histidine replacement, *Biochemistry 28*, 4791−800.
20. Linderstrøm-Lang, K. (1924) On the ionisation of proteins, *C. R. Trav. Lab. Carlsberg 15* (7), 70−95.
21. Tanford, C. (1962) The Interpretation of Hydrogen Ion Titration Curves of Proteins, *Adv. Protein Chem. 17*, 69−165.
22. Goto, Y., and Nishikori, S. (1991) Role of electrostatic repulsion in the acidic molten globule of cytochrome *c*, *J. Mol. Biol. 222*, 679−86.
23. Hagihara, Y., Tan, Y., and Goto, Y. (1994) Comparison of the conformational stability of the molten globule and native states of horse cytochrome *c*. Effects of acetylation, heat, urea and guanidine hydrochloride, *J. Mol. Biol. 237*, 336−48.
24. Tanford, C., Swanson, S. A., and Shore, W. S. (1955) Hydrogen Ion Equilibria of Bovine Serum Albumin, *J. Am. Chem. Soc. 77*, 6414−21.
25. Jamin, M., and Baldwin, R. (1998) Two Forms of the pH 4 Folding Intermediate of Apomyoglobin, *J. Mol. Biol. 276*, 491−504.
26. Santoro, M. M., and Bolen, D. W. (1988) Unfolding free energy changes determined by the linear extrapolation method. 1. Unfolding of phenylmethanesulfonyl α-chymotrypsin using different denaturants, *Biochemistry 27*, 8063−8.
27. Nishii, I., Kataoka, M., and Goto, Y. (1995) Thermodynamic stability of the molten globule states of apomyoglobin, *J. Mol. Biol. 250*, 223−38.
28. Reymond, M. T., Merutka, G., Dyson, H. J., and Wright, P. E. (1997) Folding propensities of peptide fragments of myoglobin, *Protein Sci. 6*, 706−16.
29. Nozaki, Y., and Tanford, C. (1967) Intrinsic dissociation constants of aspartyl and glutamyl carboxyl groups, *J. Biol. Chem. 242*, 4731−5.
30. Roxby, R., and Tanford, C. (1971) Hydrogen ion titration curve of lysozyme in 6 M guanidine hydrochloride, *Biochemistry 10*, 3348−52.
31. Oliveberg, M., Arcus, V. L., and Fersht, A. R. (1995) pK_A values of carboxyl groups in the native and denatured states of barnase: the pK_A values of the denatured state are on average 0.4 unit lower than those of model compounds, *Biochemistry 34*, 9424−33.
32. Springer, B. A., and Sligar, S. G. (1987) High-level expression of sperm whale myoglobin in *Escherichia coli*, *Proc. Natl. Acad. Sci. U.S.A. 84*, 8961−5.
33. Edelhoch, H. (1967) Spectroscopic determination of tryptophan and tyrosine in proteins, *Biochemistry 6*, 1948−54.
34. Luo, Y., Kay, M. S., and Baldwin, R. L. (1997) Cooperativity of folding of the apomyoglobin pH 4 intermediate studied by glycine and proline mutations, *Nat. Struct. Biol. 4*, 925−30.
35. Serrano, L., Kellis, J. T., Jr., Cann, P., Matouschek, A., and Fersht, A. R. (1992) The folding of an enzyme. II. Substructure of barnase and the contribution of different interactions to protein stability, *J. Mol. Biol. 224*, 783−804.
36. Garcia-Moreno, B., Chen, L. X., March, K. L., Gurd, R. S., and Gurd, F. R. (1985) Electrostatic interactions in sperm whale myoglobin. Site specificity, roles in structural elements, and external electrostatic potential distributions, *J. Biol. Chem. 260*, 14070−82.
37. Friend, S. H., and Gurd, F. R. (1979) Electrostatic stabilization in myoglobin. Interactive free energies between individual sites, *Biochemistry 18*, 4620−30.
38. Yang, A. S., and Honig, B. (1994) Structural origins of pH and ionic strength effects on protein stability. Acid denaturation of sperm whale apomyoglobin, *J. Mol. Biol. 237*, 602−14.
39. Cocco, M. J., Kao, Y. H., Phillips, A. T., and Lecomte, J. T. (1992) Structural comparison of apomyoglobin and metaquomyoglobin: pH titration of histidines by NMR spectroscopy, *Biochemistry 31*, 6481−91.
40. Goto, Y., Takahashi, N., and Fink, A. L. (1990) Mechanism of acid-induced folding of proteins, *Biochemistry 29*, 3480−8.

41. Matthew, J. B., and Richards, F. M. (1982) Anion binding and pH-dependent electrostatic effects in ribonuclease, *Biochemistry 21*, 4989−99.

42. Eliezer, D., and Wright, P. E. (1996) Is apomyoglobin a molten globule? Structural characterization by NMR, *J. Mol. Biol. 263*, 531−8.

43. Hollecker, M., and Creighton, T. E. (1982) Effect on protein stability of reversing the charge on amino groups, *Biochim. Biophys. Acta 701*, 395−404.

44. Staniforth, R. A., Bigotti, M. G., Cutruzzola, F., Allocatelli, C. T., and Brunori, M. (1998) Unfolding of apomyoglobin from *Aplysia limacina*: the effect of salt and pH on the cooperativity of folding, *J. Mol. Biol. 275*, 133−48.

45. Kraulis, P. (1991) MOLSCRIPT: a program to produce both detailed and schematic plots of protein structures, *J. Appl. Crystallogr. 24*, 946−950.

46. Merritt, E. A., and Murphy, M. E. P. (1994) Raster3D Version 2.0. A program for photorealistic molecular graphics, *Acta Crystallogr., Sect. D: Biol. Crystallogr. 50*, 869−73.

47. Bacon, D. J., and Anderson, W. F. (1988) A Fast Algorithm for Rendering Space-Filling Molecule Pictures, *J. Mol. Graphics 6*, 219−220.

48. Geierstanger, B., Jamin, M., Volkman, B. F., and Baldwin, R. L. (1998) Protonation Behavior of Histidine 24 and Histidine 119 in Forming the pH 4 Folding Intermediate of Apomyoglobin, *Biochemistry 37*, 4254−4265.